JCNaR
Journal of Chemical Natural Resources
Journal homepage: https://jcnar.usu.ac.id

Production of Green Diesel by Catalytic Cracking of Waste Cooking Oil Using a Bentonite Catalyst

Charles* and Minto Supeno
Department of Chemistry, Faculty of Mathematics and Natural Sciences, Universitas Sumatera Utara, Medan 20155, Indonesia
*Corresponding Author: alwicharles@gmail.com

ARTICLE INFO
Article history:
Received 18 August 2026
Revised 5 September 2026
Accepted 11 September 2026
Available online 18 September 2026

E-ISSN: 2656-1492

How to cite:
Charles and Minto Supeno. Production of Green Diesel by Catalytic Cracking of Waste Cooking Oil Using a Bentonite Catalyst. Journal of Chemical Natural Resources. 2025, 7(2):146-158.

http://doi.org/10.32734/jcnar.v7i2.27057

ABSTRACT
This study investigated the catalytic conversion of WCO using bentonite as a low-cost silica-alumina catalyst to produce a hydrocarbon-rich liquid containing green-diesel-range components. WCO was pretreated at 105 °C, while bentonite was dried at the same temperature and characterized by SEM-EDX, BET surface-area analysis, and TGA. Catalytic cracking was conducted at 350 °C using bentonite loadings of 1, 3, and 5 wt%. The liquid products were evaluated by GC-MS, FT-IR, cetane-related fuel-property analysis, and physicochemical tests. Increasing catalyst loading improved WCO conversion and liquid-product yield. At 5 wt% bentonite, the conversion and liquid-product yield reached 99.236 and 75.768 wt%, respectively, while coke formation decreased to 0.763 wt%. GC-MS showed that this product was dominated by the kerosene-range fraction (65.79%) and contained 18.25% diesel-oil-range compounds. FT-IR indicated substantial deoxygenation through decreased carbonyl intensity and disappearance of the carboxylic-acid O-H region. The product showed a cetane-related value of 48.2, viscosity of 4.93 mm^2/s, density of 862 kg/m^3, flash point of 39 °C, corrosion class 1a, and carbon residue of 0.100069% m/m. Among the investigated catalyst loadings, 5 wt% bentonite gave the best overall catalytic performance; however, the low flash point and broad product distribution indicate that further upgrading and optimization are required before the product can be considered a drop-in diesel fuel.

Keyword: Bentonite, Catalytic Cracking, Deoxygenation, Hydrocarbon-Rich Biofuel, Waste Cooking Oil

ABSTRAK
Penelitian ini mengkaji konversi katalitik minyak jelantah menggunakan bentonit sebagai katalis silika-alumina berbiaya rendah untuk menghasilkan produk cair kaya hidrokarbon yang mengandung komponen pada rentang green diesel. Minyak jelantah dipreparasi pada 105 °C, sedangkan bentonit dikeringkan pada suhu yang sama dan dikarakterisasi menggunakan SEM-EDX, analisis luas permukaan BET, dan TGA. Perengkahan katalitik dilakukan pada 350 °C dengan variasi bentonit 1, 3, dan 5 wt%. Produk cair dianalisis menggunakan GC-MS, FT-IR, analisis sifat bahan bakar terkait cetane, serta uji sifat fisika dan kimia. Pada 5 wt% bentonit diperoleh konversi 99,236 wt% dan rendemen produk cair 75,768 wt%, sedangkan pembentukan kokas menurun menjadi 0,763 wt%. Analisis GC-MS menunjukkan bahwa produk ini didominasi fraksi rentang kerosin sebesar 65,79% dan mengandung fraksi rentang diesel oil sebesar 18,25%. Hasil FT-IR menunjukkan deoksigenasi melalui penurunan intensitas karbonil dan hilangnya daerah O-H asam karboksilat. Produk memiliki nilai terkait cetane 48,2, viskositas 4,93 mm^2/s, densitas 862 kg/m^3, titik nyala 39 °C, kelas korosi 1a, dan residu karbon 0,100069% m/m. Di antara variasi katalis yang diuji, 5 wt% bentonit memberikan kinerja terbaik; namun titik nyala yang rendah dan distribusi produk yang luas menunjukkan bahwa upgrading dan optimasi lebih lanjut masih diperlukan sebelum produk dapat dipertimbangkan sebagai bahan bakar diesel drop-in.

Kata Kunci: Bentonit, Bahan Bakar Kaya Hidrokarbon, Deoksigenasi, Minyak Jelantah, Perengkahan Katalitik

1. Introduction

Indonesia's population grew by 1.13% in 2023, and population growth is accompanied by increasing energy demand. The 2022 Indonesia Energy Outlook reported that national energy consumption in 2021 increased by about 1.6% from 2020 to 123 million tonnes of oil equivalent, with transportation accounting for the largest share, followed by industry, households, and other sectors. Globally, approximately 86% of energy is still supplied by fossil fuels [1]. Because fossil fuels are non-renewable and renewable-energy generation can remain comparatively costly, sustainable and affordable alternative energy sources are required.

Waste cooking oil (WCO) is one such feedstock. It is generated by food-processing industries, households, restaurants, and other activities [2,3], with global generation from food industries and restaurants reported at approximately 41-52 Mt per year [4]. Nearly 60% of WCO may be improperly discarded, creating environmental and economic losses [5]. Treatment of improperly disposed WCO has also been associated with substantial energy and economic costs [6]. From a circular-economy perspective, WCO can therefore be viewed as a sustainable feedstock for value-added products [7]. Although collected WCO is widely used for biodiesel production, biodiesel still contains oxygenated compounds that can lower heating value, reduce storage stability, worsen cold-flow properties, and create engine-compatibility problems [8]. Biodiesel use may also increase NOx emissions [9]. These limitations motivate alternative routes that remove oxygen and produce hydrocarbon-rich green diesel.

Green diesel is obtained through catalytic conversion involving hydrodeoxygenation, decarboxylation, and decarbonylation, producing a fuel composed primarily of carbon and hydrogen [10,11]. It generally offers a relatively high cetane number, low sulfur content, and good oxidation stability [8]. Green-diesel pathways have also been reported to reduce fossil-fuel consumption and greenhouse-gas emissions [12]. However, hydrodeoxygenation can be expensive because it requires hydrogen. Decarboxylation and decarbonylation offer more economical alternatives and can operate at lower pressures and temperatures of approximately 350-500 °C, producing lighter hydrocarbons while oxygen is removed as CO2, CO, or H2O [13,14].

Catalyst development is essential because catalytic cracking can improve hydrocarbon yields and fuel quality while reducing coke formation and emissions [15]. Silica-alumina materials are particularly promising. Previous studies have demonstrated WCO or vegetable-oil cracking over nano-ZSM-5 and natural zeolite catalysts [16,17], showing that aluminosilicate acidity and pore structure can promote deoxygenation and carbon-chain cracking. Bentonite is a naturally abundant clay mineral with adsorption capacity, swelling behavior, and interlayer spaces that can provide accessible acid sites, yet its direct use as a low-cost cracking catalyst for WCO remains less studied than zeolitic systems [18]. The specific contribution of this work is therefore not the first use of a clay catalyst, but a systematic evaluation of untreated bentonite at low catalyst loadings (1, 3, and 5 wt%) under the same 350 °C cracking condition, relating catalyst loading to WCO conversion, liquid-product yield, coke formation, and hydrocarbon-fraction distribution. This approach was used to assess whether minimally processed bentonite could serve as a simple, low-cost catalyst for producing a hydrocarbon-rich biofuel from WCO.

2. Methods

2.1 Materials

The materials used were oxalic acid (Merck), distilled water, bentonite, ice, KOH (Merck), waste cooking oil, phenolphthalein, and silicone grease.

2.2 Experimental Method

2.2.1 Preparation of Waste Cooking Oil

A 100 mL portion of waste cooking oil was placed in a beaker and heated at 105 °C for 1 h. The sample was then stored in a desiccator until it reached room temperature. Before GC-MS analysis, the WCO sample underwent derivatization/sample preparation to obtain methyl-ester derivatives prior to chromatographic injection; therefore, the methyl palmitate, methyl oleate, and related methyl-ester peaks reported below refer to the derivatized analytical sample rather than to unmodified WCO. The treated oil was also characterized by FT-IR, and its acid value was determined according to SNI 01-3741-2013.

2.2.2 Preparation of the Bentonite Catalyst

Ten grams of bentonite were placed in a porcelain dish and heated at 105 °C for 1 h. The catalyst was cooled to room temperature in a desiccator and characterized by SEM-EDX, BET surface-area analysis, and

TGA. In this work, the bentonite was used in its natural form without further treatment to evaluate its potential as a low-cost catalyst with minimal pretreatment. The drying treatment was intended primarily to remove physically adsorbed moisture prior to characterization and catalytic testing.

2.2.3 Catalytic Cracking of Waste Cooking Oil

A 100 mL portion of waste cooking oil was mixed with bentonite at catalyst loadings of 1, 3, and 5 wt% using a magnetic stirrer. The mixture was transferred to a three-neck flask connected to a distillation setup and heated to 350 °C. The condensed distillate was collected and analyzed by GC-MS, FT-IR, calculated cetane number, and physical and chemical property tests.

3. Results and Discussion

3.1 Catalytic Cracking Using Bentonite

A hydrocarbon-rich liquid product was obtained by catalytic cracking of waste cooking oil at 350 °C with bentonite loadings of 1, 3, and 5 wt%. Cracking was indicated by vapor formation followed by condensation into a greenish-brown distillate. The average WCO conversions were 96.494, 97.644, and 99.236 wt%, respectively. The corresponding liquid-product yields were 46.630, 70.625, and 75.768 wt%, while coke yields were 3.505, 2.355, and 0.763 wt%. Thus, 5 wt% bentonite gave the best performance among the loadings investigated. The reaction scheme in Figure 1 is presented as a literature-based conceptual pathway rather than as direct mechanistic evidence from the present experiment [19,20]. Triglyceride hydrolysis, decarbonylation, and decarboxylation can generate hydrocarbons while removing oxygen as CO, CO_2, and H_2O. Some literature mechanisms also include hydrogenation or hydrocracking steps involving activated hydrogen [21]. However, no external H_2 was supplied in this study; therefore, hydrogen-dependent pathways were not experimentally demonstrated here and should only be regarded as possible secondary routes under conditions where hydrogen-donor species may be available.

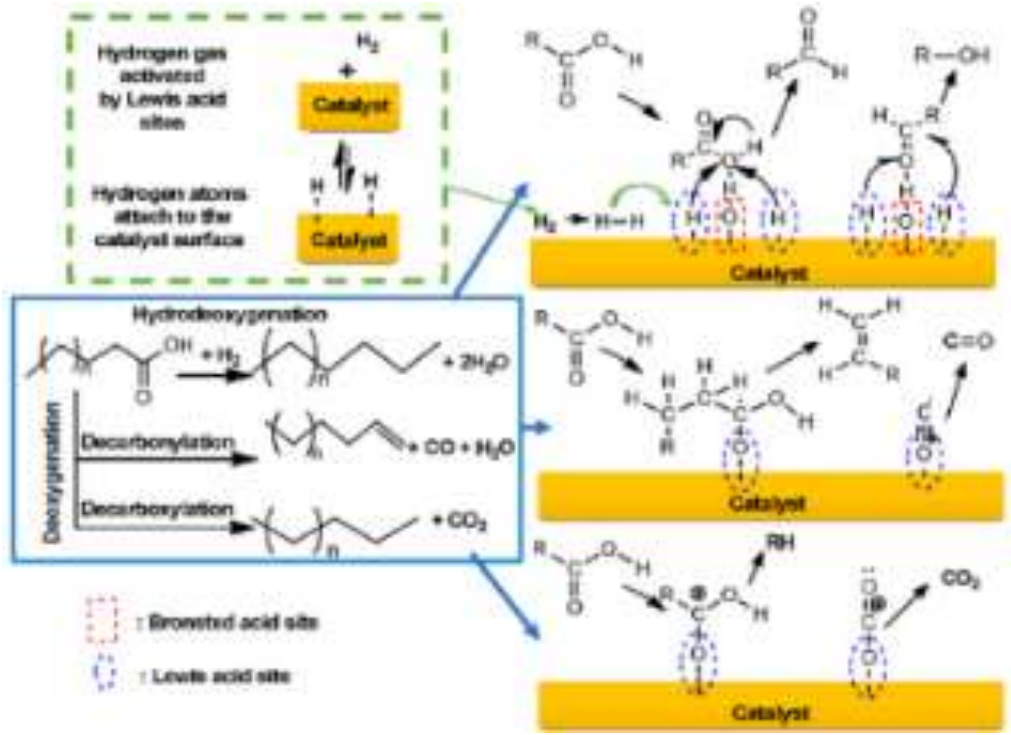

Figure 1. Proposed catalytic cracking/deoxygenation mechanism on bentonite

3.2 Reaction Pathway of Catalytic Cracking

Catalyst acidity, surface area, and pore volume are major factors that influence catalytic activity [22]. In vegetable-oil conversion, however, pore structure and the presence of suitable acid and base sites can be more important than surface area alone. Catalyst composition also affects the amount and distribution of hydrocarbon fractions [23]. Brønsted acid sites promote cracking and aromatization, whereas Lewis acid sites are associated with deoxygenation [24]. Lewis and Brønsted sites can activate hydrocarbon intermediates through carbocation chemistry [25], while metal-oxide acid-base sites can facilitate decarbonylation and decarboxylation [14]. The mechanisms illustrated in Figure 2 are therefore used to rationalize the observed

product distribution on the basis of previous studies; they were not directly verified by in situ mechanistic measurements in the present work.

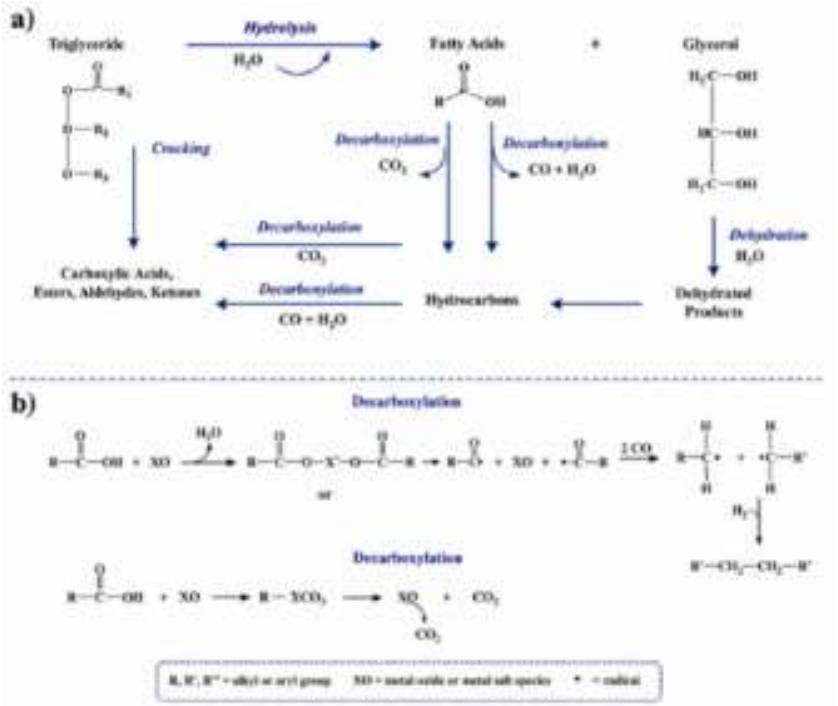

Figure 2. (a) Literature-based reaction pathway for catalytic cracking of waste cooking oil; (b) proposed decarboxylation and decarbonylation pathways on metal oxides [14].

Although the current results remain useful for interpreting the catalytic performance of bentonite, it should be noted that direct acidity characterization, such as NH_3-TPD or pyridine-FTIR analysis, could provide more comprehensive information on the acidity and the distribution of Brønsted and Lewis acid sites. Acid sites facilitate C–C and C–O bond cleavage, whereas basic sites can promote deoxygenation and suppress coke formation [26]. The synergistic combination of acid and base sites may therefore improve both cracking and deoxygenation. Catalytic cracking is commonly described by carbonium-ion/carbocation chain concepts involving initiation, propagation, and termination. In the present study, this framework is used only as a literature-based interpretation of the product chemistry and does not constitute direct identification of individual surface intermediates.

3.3 Bentonite Catalyst Characterization

3.3.1 SEM-EDX Analysis

SEM analysis (Figure 3) was used to evaluate the surface morphology and particle-shape distribution of the bentonite [27]. The SEM images showed irregular smectite layers with plate-like and honeycomb-like features that accumulated as agglomerates [28,29].

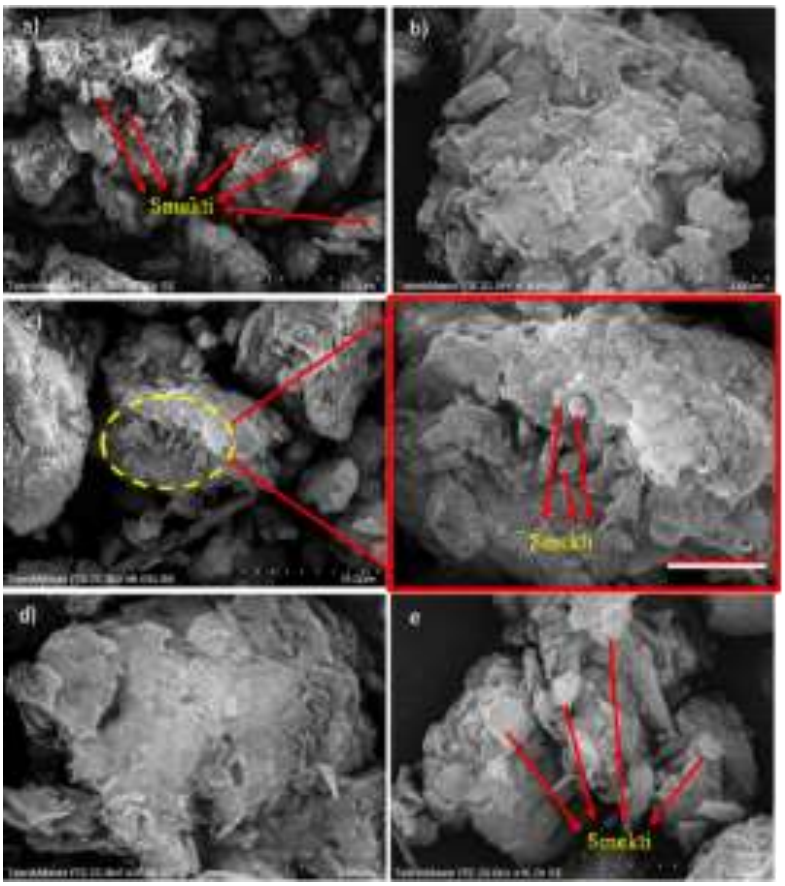

Figure 3. SEM Images of the Bentonite Catalyst

EDX characterization as can be seen in Figure 4 showed that the catalyst consisted mainly of Si (40.73 wt%), O (35.65 wt%), and Al (10.88 wt%), together with smaller amounts of Na, Mg, K, Ca, and Fe (Table 1). Moreover, it shoud be noted that the definitive identification of the mineralogical phases in natural bentonite would require complementary characterization such as X-ray diffraction (XRD).

Table 1. EDX composition of the bentonite catalyst.

Element	At (%)	Wt (%)
O	50.65	35.65
Na	1.26	1.27
Mg	0.99	1.06
Al	9.17	10.88
Si	32.96	40.73
K	0.85	1.47
Ca	1.68	2.96
Fe	2.43	5.98

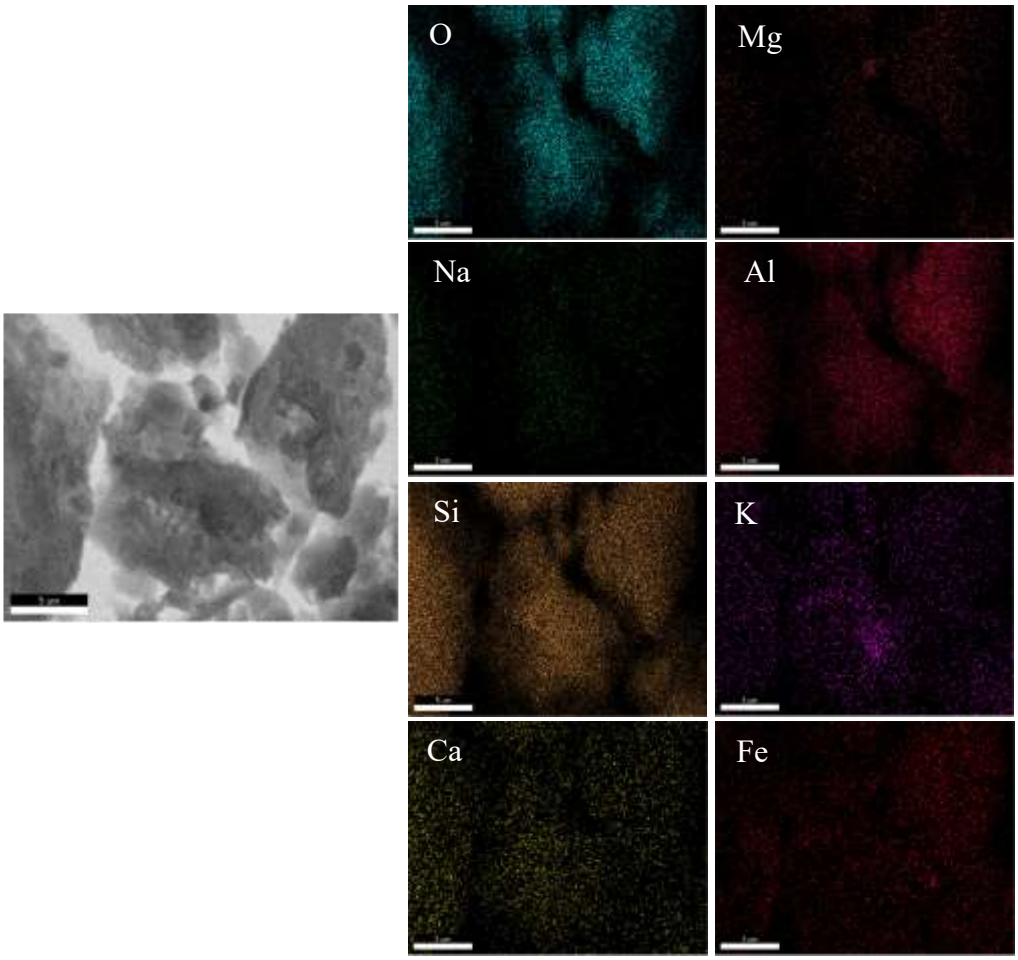

Figure 4. Elemental mapping of the bentonite catalyst.

3.3.2 BET Surface-Area Analysis

BET analysis was performed to determine the specific surface area and pore-size distribution of the bentonite. The BJH method was used to evaluate the mesopore distribution in the 2-50 nm range [30]. The adsorption-desorption isotherm was classified as type IV with an H4 hysteresis loop (Figure 5 and Table 2), indicating mesoporosity [31,32]. The pore-size distribution was approximately unimodal, and the measured surface area, total pore volume, and average pore size were 36.254 m^2/g, 0.0670249 cm^3/g, and 3.69751 nm, respectively

Table 2. Textural properties of the bentonite catalyst.

Sample	Surface area (m^2/g)	Total pore volume (cm^3/g)	Average pore size (nm)
Bentonite catalyst	36.254	0.0670249	3.69751

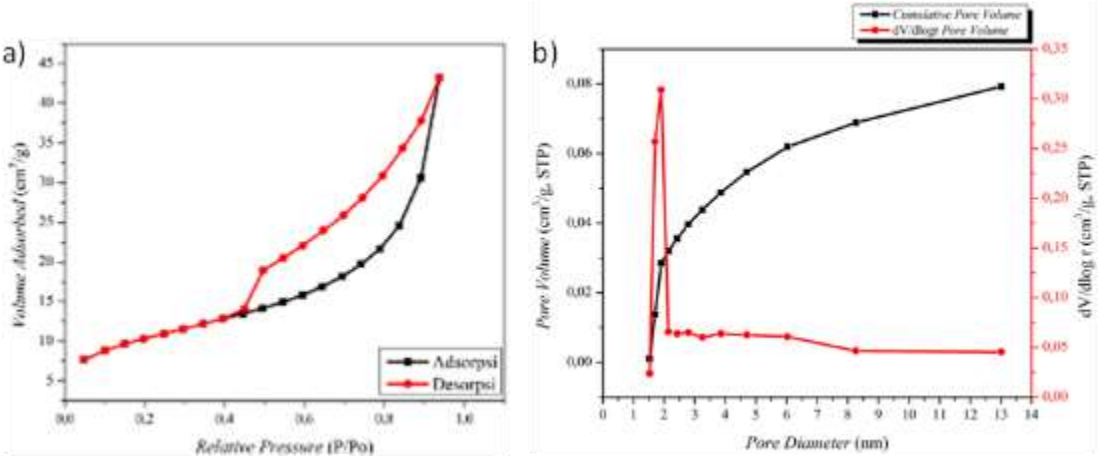

Figure 5. (a) BET adsorption-desorption isotherm and (b) BJH pore-size distribution of bentonite.

3.3.3 TGA Analysis

TGA analysis that can be seen in Figure 6 was used to evaluate the thermal stability of bentonite. Measurements were performed using a NEXTA STA-200RV under nitrogen at a flow rate of 100 mL/min. Coke formation and thermal mass loss are important because deposited coke can cover active sites and reduce catalytic activity [24]. Acid strength may also influence coke production, and mesopores can affect molecular diffusion to acid sites [35].

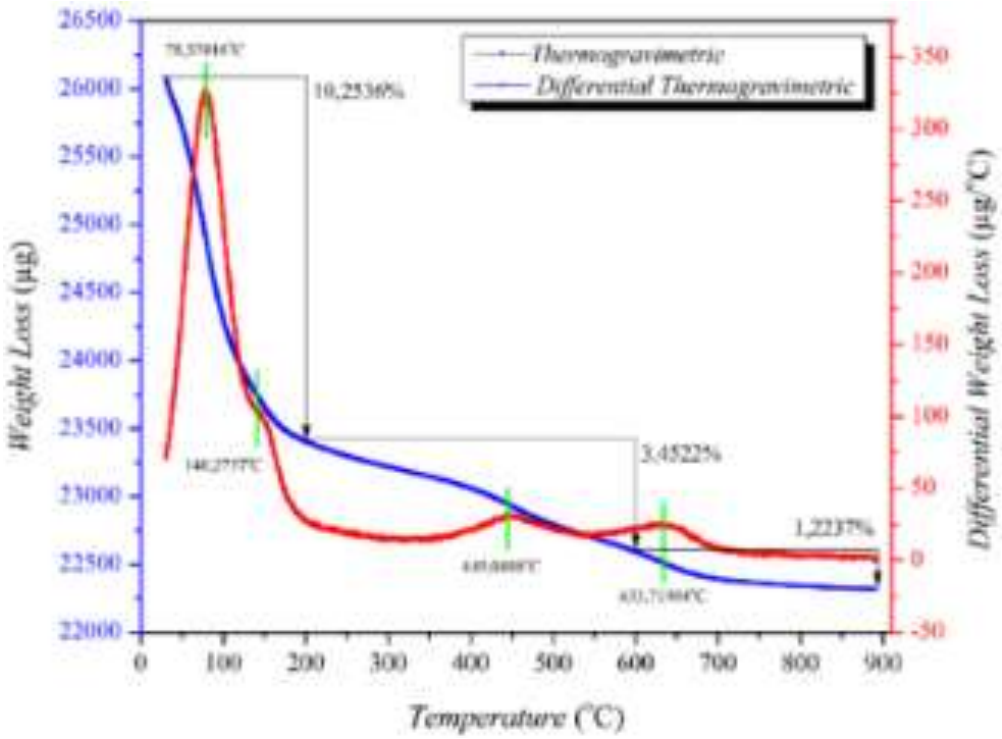

Figure 6. TGA profile of the bentonite catalyst.

The bentonite showed multistage decomposition. Between approximately 78 and 200 °C, a 10.2536% mass loss was attributed mainly to dehydration [34]. From 200 to 600 °C, a further 3.4522% loss was associated with removal of residual lattice water, dehydroxylation, and structural changes in the silica-alumina layers [35,36]. Above 600 °C, an additional 1.2237% loss indicated progressive chemical decomposition; temperatures above about 700 °C were considered damaging to the bentonite structure [37].

3.4 Characterization of Waste Cooking Oil

3.4.1 GC-MS Analysis

The composition of WCO (Figure 7) was analyzed using a Shimadzu GCMS-QP2010S with an Rtx-5MS column (30 m × 0.25 mm, 0.25 µm film thickness). Helium was used as the carrier gas at 0.50 mL/min and 13.7 kPa; the column-oven and injector temperatures were 70 and 300 °C, respectively. The chromatogram indicated fatty-acid-related components including oleic, palmitic, stearic, myristic, and lauric derivatives.

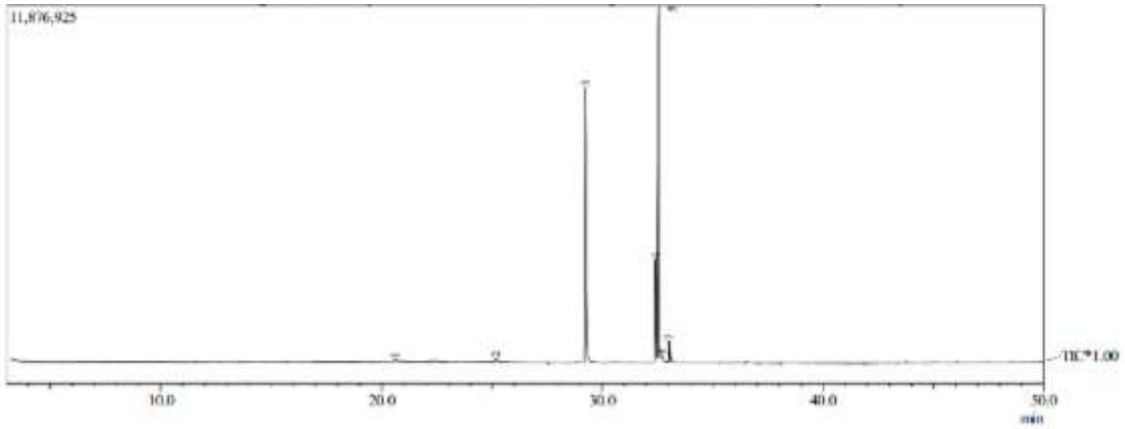

Figure 7. GC-MS chromatogram of the derivatized waste cooking oil sample.

Table 3. GC-MS components of the derivatized waste cooking oil sample.

Retention time (s)	Compound	Molecular formula	Selectivity (%)
20.592	Methyl dodecanoate	$C_{13}H_{26}O_2$	0.22
25.180	Methyl tetradecanoate	$C_{15}H_{30}O_2$	0.60
29.238	Methyl palmitate	$C_{17}H_{34}O_2$	37.52
32.410	9,12-Hexadecadienoic acid	$C_{16}H_{28}O_2$	11.92
32.548	Methyl oleate	$C_{19}H_{36}O_2$	44.52
32.673	Methyl oleate	$C_{19}H_{36}O_2$	1.90
33.051	Methyl stearate	$C19H_{38}O_2$	3.33

The total saturated-fatty-acid-related fraction determined by GC-MS was 41.67%. Compared with the limits cited from SNI 3741:2013 for edible cooking oil, this composition was considered outside the specification and supported classification of the sample as waste cooking oil.

3.4.2 FT-IR Analysis

FT-IR (Figure 8) characterization was performed using a Shimadzu IRPrestige-21 with an attenuated total reflectance accessory. The WCO spectrum (Table 4) showed an ester C=O stretching band at 1743.65 cm−1, together with C=O overtone and C-O-C stretching bands at 3469.94 and 1238.30-1116.78 cm−1. A band at 3005.09 cm−1 was assigned to =C-H sp^2 stretching, while bands at 2922.16 and 2852.72 cm−1 were assigned to asymmetric and symmetric sp^3 C-H stretching of CH2. Additional bands at 1463.97 and 1375.25 cm−1 were assigned to CH_2 and CH_3 bending, and the band at 723.31 cm−1 indicated long-chain -(CH_2)n- groups.

Table 4. FT-IR bands of waste cooking oil.

Wavenumber (cm^{-1})	Assignment
3469.94	C=O overtone
3005.09	=C-H sp^2 stretching
2922.16	Asymmetric sp^3 C-H stretching of CH_2
2852.72	Symmetric sp^3 C-H stretching of CH_2
1743.65	Ester C=O stretching
1658.78	C=C stretching (trans)
1463.97	sp^3 C-H bending of CH_2
1375.25	sp^3 C-H bending of CH_3
1238.30-1116.78	C-O-C stretching
966.34-873.75	=C-H sp^2 out-of-plane bending
723.31	-(CH_2)n-, n>4 rocking

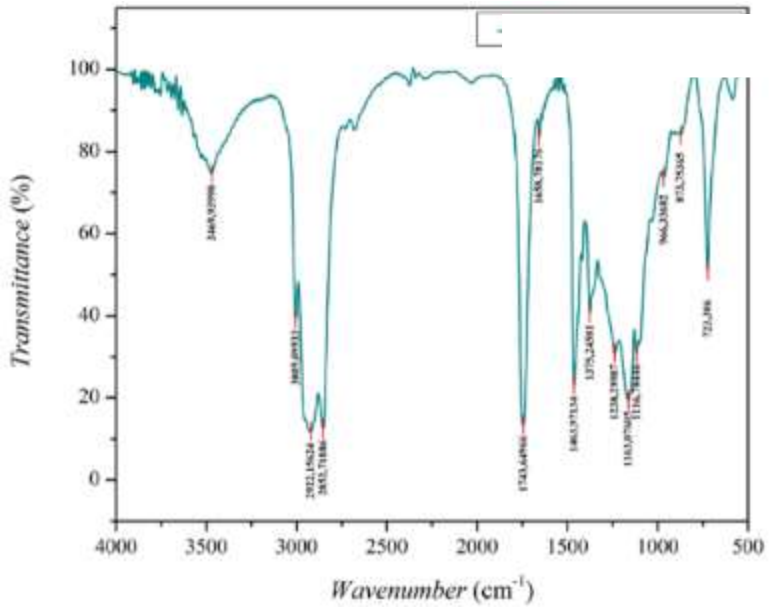

Figure 8. FT-IR spectrum of waste cooking oil.

3.4.3 Total Acid Value

The acid value (Table 5) was determined by alkalimetric titration according to SNI 3741:2013. KOH volumes of 3.50, 3.75, and 4.00 mL were required in three replicates, giving an average acid value of 2.096 mg KOH/g. This value was higher than the 0.6 mg KOH/g limit cited for cooking oil, further supporting classification of the sample as waste cooking oil.

Table 5. Acid-value titration data for waste cooking oil.

Replicate	KOH volume (mL)	KOH normality (N)	Oil mass (g)
1	3.50	0.100	10.079
2	3.75	0.100	10.006
3	4.00	0.100	10.017
Average	3.75	0.100	10.034

3.5 Characterization of the Hydrocarbon-Rich Liquid Product

3.5.1 GC-MS Analysis

The hydrocarbon-rich liquid products were analyzed using a Shimadzu GCMS-QP2010S with an Rxi-1ms column (30 m × 0.25 mm, 0.25 µm film thickness). Helium was used at 3 mL/min and 100 kPa, with column-oven and injector temperatures of 60 and 200 °C, respectively. Without catalyst, the oxygenated-hydrocarbon fraction dominated at 58.68%. With bentonite loadings of 1, 3, and 5 wt%, the kerosene-range fraction increased to 51.54, 58.84, and 65.79%, respectively (Figure 9 and Table 6). At 5 wt% bentonite, the diesel-oil-range fraction was 18.25%. Accordingly, the condensate is more accurately described as a hydrocarbon-rich biofuel or green-diesel-containing liquid product rather than a compositionally pure green diesel.

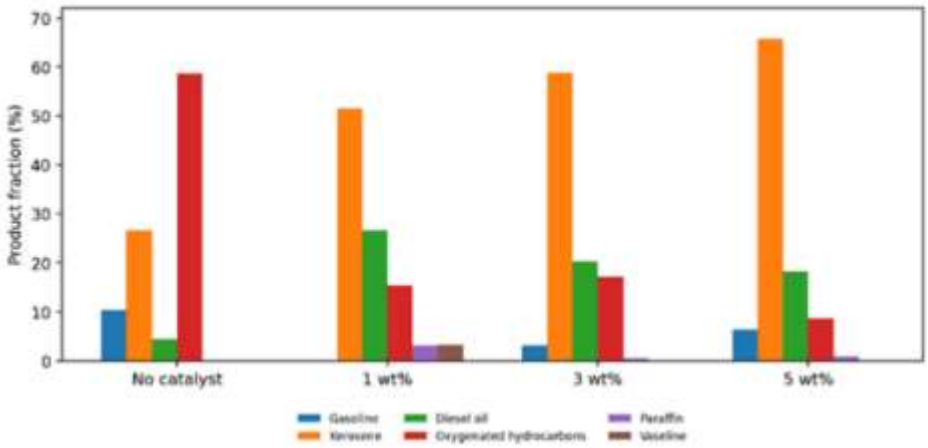

Figure 9. GC-MS product-fraction distribution of the hydrocarbon-rich liquid at different bentonite loadings.

Table 6. GC-MS product fractions of the hydrocarbon-rich liquid.

Fraction	No catalyst	1 wt%	3 wt%	5 wt%
Gasoline	10.28	0	3.11	6.45
Kerosene	26.68	51.54	58.84	65.79
Diesel oil	4.36	26.65	20.29	18.25
Oxygenated hydrocarbons	58.68	15.38	17.22	8.61
Paraffin	0	3.17	0.54	0.90
Vaseline	0	3.26	0	0

3.5.2 FT-IR Analysis

FT-IR analysis (Figure 10) of the hydrocarbon-rich liquid products showed a decrease in the C=O stretching intensity in the 1700–1750 cm^{-1} region, a characteristic C–(C=O)–C vibration in the 1300–1000 cm^{-1} region, and disappearance of the broad carboxylic-acid O–H stretching region at 3400–2400 cm^{-1} (Table 7). These changes indicate substantial deoxygenation and cleavage of carboxylic-acid functionalities during catalytic cracking.

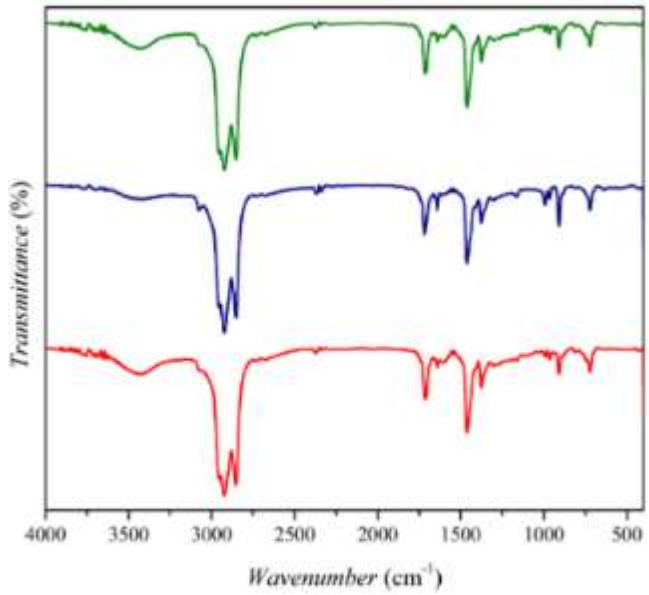

Figure 10. FT-IR spectra of the hydrocarbon-rich liquid products obtained using 1, 3, and 5 wt% bentonite.

Table 7. FT-IR bands of the hydrocarbon-rich liquid product.

Wavenumber (cm^{-1})	Assignment
3427.51	C=O overtone
3076.46	=C-H sp^2 stretching
2954.95	sp^3 C-H stretching
2924.09	Asymmetric sp^3 C-H stretching of CH2
2852.72	Symmetric sp^3 C-H stretching of CH2
1718.58	Ketone C=O stretching with α,β-C=C
1641.42	C=C stretching (trans)
1462.04	sp^3 C-H bending of CH2
1375.25-1301.95	sp^3 C-H bending of CH3
1163.08	C-(C=O)-C bending
993.34-908.47	=C-H sp^2 out-of-plane bending
721.38	-(CH2)n-, n>4 rocking

3.5.3 Physical and Chemical Properties of the 5 wt% Bentonite Product

Physical and chemical properties (Table 8) were evaluated to assess the fuel-like characteristics of the product [38]. The product obtained with 5 wt% bentonite had a calculated cetane index of 48.2 (ASTM D4737) [39], viscosity of 4.93 mm^2/s (ASTM D445), density of 862 kg/m^3 (ASTM D4052) [40], carbon residue of 0.100069% m/m (ASTM D189), copper-strip corrosion class 1a (slight tarnish) (ASTM D130), and flash point of 39 °C (ASTM D93). The measured flash point of 39 °C is an important limitation. For comparison, ASTM D975 specifies a minimum flash point of 52 °C for No. 2-D diesel fuel using ASTM D93 [41]. Therefore, the obtained product does not satisfy this diesel flash-point criterion and should be considered a hydrocarbon-rich biofuel intermediate that requires further fractionation or upgrading before practical use as a diesel-like fuel.

Table 8. Physical and chemical properties of the hydrocarbon-rich liquid product obtained with 5 wt% bentonite.

Characteristic	Unit	Method	Result
Calculated cetane index	-	ASTM D4737	48.2
Viscosity	mm^2/s	ASTM D445	4.93
Density	kg/m^3	ASTM D4052	862
Carbon residue	% m/m	ASTM D189	0.100069
Corrosion	-	ASTM D130	1a (slight tarnish)
Flash point	°C	ASTM D93	39

4. Conclusion

Bentonite showed an agglomerated smectite-layer morphology and was composed mainly of Si (40.73 wt%), O (35.65 wt%), and Al (10.88 wt%). Increasing the bentonite loading from 1 to 5 wt% increased WCO conversion from 96.494 to 99.236 wt% and liquid-product yield from 46.630 to 75.768 wt%, while coke yield decreased from 3.505 to 0.763 wt%. At 5 wt% bentonite, GC-MS showed a kerosene-range fraction of 65.79%, a diesel-oil-range fraction of 18.25%, oxygenated hydrocarbons of 8.61%, gasoline of 6.45%, and paraffin of 0.90%. FT-IR results supported substantial deoxygenation. Among the catalyst loadings investigated, 5 wt% bentonite gave the best overall performance; this result should not be interpreted as a globally optimized condition because catalyst loadings above 5 wt%, other temperatures, residence times, and catalyst modifications were not evaluated. Moreover, the 39 °C flash point and the dominance of the kerosene-range fraction show that the condensate is better described as a hydrocarbon-rich, green-diesel-containing biofuel intermediate rather than a finished drop-in diesel fuel. Further optimization, fractionation, upgrading, and standardized fuel testing are therefore required.

References

[1] Gautam P, Kumar S, Lokhandwala S. Energy-aware intelligence in megacities. In Current Developments in Biotechnology and Bioengineering: Waste Treatment Processes for Energy Generation (pp. 211–238). Elsevier 2019. doi:10.1016/B978-0-444-64083-3.00011-7.

[2] Thushari I, Babel S. Comparative study of the environmental impacts of used cooking oil valorization options in Thailand. Journal of Environmental Management, 310 2022. doi:10.1016/j.jenvman.2022.114810.
[3] Chen C, Chitose A, Kusadokoro M, Nie H, Xu W, Yang F, Yang S. Sustainability and challenges in biodiesel production from waste cooking oil: An advanced bibliometric analysis. Energy Reports, 7, 4022–4034 2021. doi:10.1016/j.egyr.2021.06.084.
[4] Orjuela A, Clark J. Green chemicals from used cooking oils: Trends, challenges, and opportunities. Current Opinion in Green and Sustainable Chemistry (Vol. 26). Elsevier B.V 2020. doi:10.1016/j.cogsc.2020.100369.
[5] Zhao Y, Wang C, Zhang L, Chang Y, Hao Y. Converting waste cooking oil to biodiesel in China:Environmental impacts and economic feasibility. Renewable and Sustainable Energy Reviews, 140. 15 2021.
[6] Frota de Albuquerque Landi F, Fabiani C, Castellani B, Cotana F, Pisello AL. Environmental assessment of four waste cooking oil valorization pathways. Waste Management, 138, 219–233 2022. doi:10.1016/j.wasman.2021.11.037.
[7] Liepins J, Balina K, Soloha R, Berzina I, Lukasa LK, Dace E. Glycolipid biosurfactant production from waste cooking oils by yeast: Review of substrates, producers and products. In Fermentation (Vol. 7, Issue 3). MDPI AG 2021. doi:10.3390/fermentation7030136.
[8] Kamaruzaman MF, Taufiq-Yap YH, Derawi D. Green diesel production from palm fatty acid distillate over SBA-15-supported nickel, cobalt, and nickel/cobalt catalysts. Biomass and Bioenergy, 134 2020. doi:10.1016/j.biombioe.2020.105476.
[9] Murnieks R, Apseniece L, Kampars V, Shustere Z, Malins K. Investigation of Deoxygenation of Rapeseed Oil over Raney Nickel and Ni/SiO2−Al2O3 Catalysts. Arabian Journal for Science and Engineering, 41(6), 2193–2198 2016. doi:10.1007/s13369-015-1932-2.
[10] Nugrahaningtyas KD, Lukitawati R, Mukhsin SA, Fadlulloh Z, Sabiilagusti AI, Budiman AW, Kurniawati MF. Conversion of waste cooking oil into green diesel using Ni/MOR and Cu/MOR catalysts. Journal of Physics: Conference Series, 2190(1) 2022. doi:10.1088/1742-6596/2190/1/012037.
[11] Baharudin KB, Abdullah N, Taufiq-Yap YH, Derawi D. Renewable diesel via solventless and hydrogen-free catalytic deoxygenation of palm fatty acid distillate. Journal of Cleaner Production, 274 2020. doi:10.1016/j.jclepro.2020.122850.
[12] Douvartzides SL, Charisiou ND, Papageridis KN, Goula MA. Green diesel: Biomass feedstocks, production technologies, catalytic research, fuel properties and performance in compression ignition internal combustion engines. Energies (Vol. 12, Issue 5). MDPI AG 2019. doi:10.3390/en12050809.
[13] Asikin N, Lee HV, Alsultan GA, Yap T. Synthesis and characterization of silicaalumina supported Ca and Ni catalyst for deoxygenation of vegetable oil into diesel. Materials Science Forum, 840, 353–358 2016. doi:10.4028/www.scientific.net/MSF.840.353.
[14] Thangadurai T, Tye CT. Acidity and basicity of metal oxide-based catalysts in catalytic cracking of vegetable oil. In Brazilian Journal of Chemical Engineering (Vol. 38, Issue 1). Springer Science and Business Media Deutschland GmbH 2021. doi:10.1007/s43153-02000085-z.
[15] Rabie AM, Mohammed EA, Negm NA. Feasibility of modified bentonite as acidic heterogeneous catalyst in low temperature catalytic cracking process of biofuel production from nonedible vegetable oils. Journal of Molecular Liquids, 254, 260–266 2018. doi:10.1016/j.molliq.2018.01.110.
[16] Wang S, Jiang X, Nie G, Wang Z, Yu H, Liu Y, Wu Q, Yu S, Liu S. Trash into treasure: Nano ZSM-5 catalyst for cracking waste cooking oil to bio-gasoline with enhanced selectivity. Fuel Processing Technology, 242 2023. doi:10.1016/j.fuproc.2023.107666.
[17] Aziz I, Adhani L, Yolanda T, Saridewi N. Catalytic cracking of Jatropa curcas oil using natural zeolite of Lampung as a catalyst. IOP Conference Series: Earth and Environmental Science, 299(1) 2019. doi:10.1088/1755-1315/299/1/012065.
[18] Hamouda AS, Acharjee P, Abdelrahman A, Radwan AM, Zaki AH, Farghali A, Mohamed HFM, Yadav A, Bhatnagar A, Goel A. Catalytic thermochemical cracking of polyethylene over nanocomposite bentonite clay. IOP Conference Series: Materials Science and Engineering, 1046(1), 012022 2021. doi:10.1088/1757-899x/1046/1/012022.
[19] Istadi I, Riyanto T, Khofiyanida E, Buchori L, Anggoro DD, Sumantri I, Putro BHS, Firnanda AS. Low-oxygenated biofuels production from palm oil through hydrocracking process using the enhanced Spent RFCC catalysts. Bioresource Technology Reports, 14 2021. doi:10.1016/j.biteb.2021.100677.
[20] Istadi I, Riyanto T, Buchori L, Anggoro DD, Gilbert G, Meiranti KA, Khofiyanida E. Enhancing Brønsted and Lewis Acid Sites of the Utilized Spent RFCC Catalyst Waste for the Continuous Cracking Process of

Palm Oil to Biofuels. Industrial and Engineering Chemistry Research, 59(20), 9459–9468 2020. doi:10.1021/acs.iecr.0c01061.
[21] Li Y, Hou C, Jiang J, Zhang Z, Zhao C, Page AJ, Ke Z. General H2 Activation Modes for Lewis Acid-Transition Metal Bifunctional Catalysts. ACS Catalysis, 6(3), 1655–1662 2016. doi:10.1021/acscatal.5b02395.
[22] Zhao X, Wei L, Cheng S, Julson J. Review of heterogeneous catalysts for catalytically upgrading vegetable oils into hydrocarbon biofuels. In Catalysts (Vol. 7, Issue 3). MDPI 2017. doi:10.3390/catal7030083.
[23] Asikin-Mijan N, Lee HV, Abdulkareem-Alsultan G, Afandi A, Taufiq-Yap YH. Production of green diesel via cleaner catalytic deoxygenation of Jatropha curcas oil. Journal of Cleaner Production, 167, 1048–1059 2017. doi:10.1016/j.jclepro.2016.10.023.
[24] Ahmad M, Farhana R, Raman AAA, Bhargava SK. Synthesis and activity evaluation of heterometallic nano oxides integrated ZSM-5 catalysts for palm oil cracking to produce biogasoline. Energy Conversion and Management, 119, 352–360 2016. doi:10.1016/j.enconman.2016.04.069.
[25] Almutairi SMT, Mezari B, Filonenko GA, Magusin PCMM, Rigutto MS, Pidko EA, Hensen EJM. Influence of Extraframework Aluminum on the Brønsted Acidity and Catalytic Reactivity of Faujasite Zeolite. ChemCatChem, 5(2), 452–466 2013. doi:10.1002/cctc.201200612.
[26] Abdulkareem-Alsultan G, Asikin-Mijan N, Mustafa-Alsultan G, Lee HV, Wilson K, Taufiq-Yap YH. Efficient deoxygenation of waste cooking oil over Co3O4-La2O3-doped activated carbon for the production of diesel-like fuel. RSC Advances, 10(9), 4996–5009 2020. doi:10.1039/c9ra09516k.
[27] Jawad AH, Saber SEM, Abdulhameed AS, Farhan AM, ALOthman ZA, Wilson LD. Characterization and applicability of the natural Iraqi bentonite clay for toxic cationic dye removal: Adsorption kinetic and isotherm study. Journal of King Saud University - Science, 35(4) 2023. doi:10.1016/j.jksus.2023.102630.
[28] Lee JH, Kim J, Kwon JS, Jo HY. Effect of hydrothermal alteration of Cabentonite in K-rich solutions with different pHs on the physicochemical, swelling, and Cs adsorption properties. Applied Geochemistry, 158 2023. doi:10.1016/j.apgeochem.2023.105791.
[29] Maged A, Kharbish S, Ismael IS, Bhatnagar A. Characterization of activated bentonite clay mineral and the mechanisms underlying its sorption for ciprofloxacin from aqueous solution. Environmental Science and Pollution Research, 27(26), 32980–32997 2020. doi:10.1007/s11356-020-09267-1.
[30] Yang Y, Zhang J, Xu L, Li P, Liu Y, Dang W. Pore Structure and Fractal Characteristics of Deep Shale: A Case Study from Permian Shanxi Formation Shale, from the Ordos Basin. ACS Omega, 7(11), 9229–9243 2022. doi:10.1021/acsomega.1c05779.
[31] Noskov AV, Alekseeva OV, Shibaeva VD, Agafonov AV. Synthesis, structure and thermal properties of montmorillonite/ionic liquid ionogels. RSC Advances, 10(57), 34885–34894 2020. doi:10.1039/d0ra06443b.
[32] Amaya J, Bobadilla L, Azancot L, Centeno M, Moreno S, Molina R. Potentialization of bentonite properties as support in acid catalysts. Materials Research Bulletin, 123 2020. doi:10.1016/j.materresbull.2019.110728.
[33] Muhammad I, Makwashi N, Ahmed TG, Manos G, Zhao D. A Mechanistic Model on Catalyst Deactivation by Coke Formation in a CSTR Reactor. Processes, 11(3) 2023. doi:10.3390/pr11030944.
[34] Widjaya RR, Juwono AL, Rinaldi N. Bentonite modification with pillarization method using metal stannum. AIP Conference Proceedings, 1904 2017. doi:10.1063/1.5011867.
[35] Baloyi J, Ntho T, Moma J. Synthesis of highly active and stable Al/Zr pillared clay as catalyst for catalytic wet oxidation of phenol. Journal of Porous Materials, 26(2), 583–597 2019. doi:10.1007/s10934-018-0667-3.
[36] Widjaya RR, Saridewi N, Putri AA, Rinaldi N, Dwiatmoko AA. Fe-Cr pillared clay as catalysts for the ethanol to gasoline conversion. IOP Conference Series: Materials Science and Engineering, 1011(1) 2021. doi:10.1088/1757-899X/1011/1/012008.
[37] Olegario EM, Gili MBZ. Characterization of Philippine natural bentonite. Experimental Results, 2 2021. doi:10.1017/exp.2021.16.
[38] Mofijur M, Rasul MG, Hassan NMS, Masjuki HH, Kalam MA, Mahmudul HM. Assessment of physical, chemical, and tribological properties of different biodiesel fuels. In Clean Energy for Sustainable Development: Comparisons and Contrasts of New Approaches (pp. 441–463). Elsevier Inc 2017. doi:10.1016/B978-0-12-805423-9.00014-4.